buildings

MDPI

Article

Modified Lime Binders for Restoration Work

Valentina Loganina [1], Kristina Sergeeva [1], Roman Fediuk [2,*], Sergey Klyuev [3], Nikolai Vatin [4] and Yuriy Vasilev [5]

[1] Penza State University of Architecture and Construction, 440028 Penza, Russia; loganin@mail.ru (V.L.); papsheva.ka@gmail.com (K.S.)
[2] Polytechnic Institute, Far Eastern Federal University, 690922 Vladivostok, Russia
[3] Department of Theoretical Mechanics and Strength of Materials, Belgorod State Technological University named after V.G. Shukhov, 308012 Belgorod, Russia; klyuyev@yandex.ru
[4] Peter the Great St. Petersburg Polytechnic University, 195251 St. Petersburg, Russia; vatin@mail.ru
[5] Moscow Automobile and Road Construction University, 125319 Moscow, Russia; yu.vasilev@madi.ru
* Correspondence: fedyuk.rs@dvfu.ru

Abstract: Lime mixes are the primary material for restoration work in historic buildings. The research object of this study is modifying lime binders with specially synthesized calcium silicate hydrates (CSHs). This study aimed to improve lime render mixes' weather resistance. The following factors were considered: the density of the liquid glass, the amount of the precipitating additive, the rate of introduction of the precipitating additive, the drying mode of the precipitate, and the storage time of the precipitate. The research methods were X-ray diffraction analysis, differential thermal analysis, Fourier transform infrared spectrometry, and optical and electron microscopy. It was revealed that lime compositions with CSH have a higher strength gain rate than the control compositions. A mathematical model of the kinetics of hardening a lime composite based on a binder filled with CSH was obtained. The regularities of the change in the lime composite's strength depending on the filler grinding's fineness, its content, and the amount of mixing water have been established. It was revealed that the introduction of CSH into the lime composition increases the weather resistance of facade lime mixtures by reducing the porosity and increasing the volume of closed pores of the composite.

Keywords: lime; calcium silicate hydrates; modification; restoration mix

check for updates

Citation: Loganina, V.; Sergeeva, K.; Fediuk, R.; Klyuev, S.; Vatin, N.; Vasilev, Y. Modified Lime Binders for Restoration Work. *Buildings* **2021**, *11*, 98. https://doi.org/10.3390/buildings11030098

Academic Editors: Paula Lopez-Arce and Ainara Zornoza-Indart

Received: 2 February 2021
Accepted: 2 March 2021
Published: 5 March 2021

1. Introduction

For the restoration of buildings and structures of historical development and the decoration of newly erected objects, dry plaster and render mixes are widely used [1,2]. The production of dry mixes is one of the most rapidly developing construction industry areas and one of the largest construction market segments [3,4]. Since 2015, the construction sector has seen an increase in production of dry plaster and render mixes by 10–25% [5]. The volume of production of plaster, render and putty mixtures is increasing every year, and today it is about 48% of the production of dry mixes [6,7].

The traditional materials used for the finishing and renovation of facades for many years have been lime compounds [8,9]. Lime dry render mixes are used mainly to restore architectural monuments and buildings since restoration of historical buildings causes certain difficulties associated with lime render incompatibility with finishing materials [10,11]. Additionally, lime compositions are characterized by higher fracture toughness compared to cement ones [12,13]. In particular, the ratio of flexural strength to compressive strength for cement materials is 0.1–0.15, and for lime compositions, this ratio is 4–6 times higher, amounting to 0.6 [14,15]. However, coatings based on lime-based dry mixes are characterized by low water resistance, which leads to increased costs [16]. In this regard, it is urgent to develop a technological solution that increases coatings' durability based on lime dry mixes [17–19].

To increase the water resistance of lime coatings, Pahlavan et al. [20] propose the introduction of hydrophobic additives to the mix formulation, which, having an air entrainment of 3–5%, form a network of closed pores. Accordingly, the stresses arising from the freezing of water in open pores decrease, thereby significantly increasing the coatings' frost resistance [21–23].

Another way to improve performance is the use of active mineral additives. In particular, the use of mineral additives leads to an increase in water resistance, impermeability and chemical resistance, an improvement in crack resistance, and an increase in compressive strength [24,25]. High activity fillers increase the adhesion of solutions based on dry building mixes with the base [26,27]. Natural additives (silica, alumina, trepel, opoka, diatomite, ashes, tuffs, pumice, volcanic ash) and artificial additives (granulated blast-furnace slags, fuel ash, and slag, artificially fired clay materials, silica waste) are used [28]. The interaction of lime with active mineral additives is based on the fact that active (amorphous and finely dispersed) silica binds lime in the presence of water [29]. As a result of this reaction, calcium silicate hydrates are formed, determining the hydraulic hardening of lime—i.e., strength build-up under water after prehardening in air [30]. In addition to silica, the active mineral additives contain alumina, which in the presence of moisture can also interact with lime, forming calcium hydroaluminate with hydraulic properties [31].

The use of calcium silicate hydrate (CSH) additives to enhance the performance of limestone formulations is much less studied.

In this regard, as a scientific hypothesis, an assumption was made about the possibility of increasing the operational resistance of lime finishing coatings by introducing active fillers based on calcium silicate hydrates into dry render mix formulations.

The study aimed to improve lime render mixes' weather resistance by modifying lime binders with specially synthesized calcium silicate hydrates. The following tasks were solved to achieve this goal:

- studying of the regularities of the synthesis of finely dispersed fillers based on calcium silicate hydrates;
- researching of the structure formation of lime systems in the presence of CSH fillers.

2. Materials and Methods

2.1. Characteristics of the Used Raw Materials

The initial binder was lime (Atmis-sugar, Russian Federation) with an activity of 75–84%, a real density of 2205 kg/m^3, a bulk density of 500 kg/m^3, and a specific surface area of 10,000 cm^2/g. Liquid sodium glass with a different silicate modulus and calcium chloride $CaCl_2$, which acted as a precipitant, was used to obtain filler based on CSH. The amount of added precipitant was 30–50% by weight of water glass. The precipitant was added as a 7.5–15% water solution, depending on the density and silicate modulus of water glass. A silicate modulus of water glass was calculated as the ratio of the number of grams of silicon dioxide molecules to the number of grams of sodium oxide molecules.

The binders were mixed with drinking water with a pH of 7.12.

Superplasticizers were introduced into the mix formulation to regulate the finished compositions' rheological, mechanical, and functional properties. The superplasticizers were: K (a mixture of sodium salts of polymethylene naphthalenesulfonic acids with a high content of high molecular weight fractions), P-4 (based on methylene naphthalenesulfonate, as well as organic and inorganic sodium compounds), S-3 (sulfonated naphthalene-formaldehyde polycondensates), SP-3 (a mixture of sodium salts of polymethylene naphthalenesulfonic acids of various molecular weights), F15G (sulfonated melamine-based polycondensation powder) and 1641F (polycarboxylate ether). The amount of additive was 0.7–2% by weight of the binder.

For comparison, mineral additives such as silica fume, wollastonite and diatomite were used (Table 1).

Table 1. Chemical composition of mineral additives.

Mineral Additive	SiO_2	Fe_2O_3	Al_2O_3	CaO	MgO	K_2O	Na_2O	LOI
Diatomite	79.1	4.1	9.3	1.0	1.0	0.2	0.4	4.4
Wollastonite	53.4	2.4	3.1	34.7	0.3	-	-	6.4
Silica fume	86.8	1.0	0.8	0.3	1.5	1.7	0.8	1.6

2.2. Mix Design

The mixes were designed with different ratios of synthesized CSH added to lime and different ratios of water to lime (Table 2). For comparison, other mineral additives such as silica fume (SF), wollastonite (W) and diatomite (D) were added to the lime mix.

Table 2. Mix design.

Mix ID	Composition	Water-Lime Ratio
Ref-A	lime	0.7
Ref-B		0.9
005-A	lime:CSH = 1:0.05	0.7
005-B		0.9
015-A	lime:CSH = 1:0.15	0.7
015-B		0.9
03-A	lime:CSH = 1:0.3	0.7
03-B		0.9
03-D		1.2
05-B	lime:CSH = 1:0.5	0.9
05-C		1.0
05-D		1.2
03D-B	lime:D = 1:0.3	0.9
01-02D-B	lime:CSH:D = 1:0.1:0.2	0.9
02-01D-B	lime:CSH:D = 1:0.2:0.1	0.9
03W-A	lime:W = 1:0.3	0.7
03W-B		0.9
015W-A	lime:W = 1:0.15	0.7
015W-B		0.9
03SF-A	lime:SF = 1:0.3	0.7
03SF-B		0.9
015SF-A	lime:SF = 1:0.15	0.7
015SF-B		0.9

2.3. Laboratory Equipment and Research Methods

The obtained filler’s granulometric composition was assessed using an Analysette 22 automatic laser diffractometer (Fritsch, Idar-Oberstein, Germany). The determination of the specific surface area of powder materials was carried out by air permeability on a PSH-11 device (Stroydetal, Moscow, Russia). XRD patterns of the studied samples were obtained on an ARL X’TRA diffractometer (Thermo Electron, Waltham, MA, USA). SEM images were obtained using a G2 pro scanning electron microscope (Phenom-world BV, Eindhoven, The Netherlands). Images of CSH crystals were also obtained using an optical microscope (Nikon, Tokyo, Japan). IR spectrometry was carried out using a 1000 FT-IR instrument (Varian Scimitar, Palo Alto, USA). Differential thermal analysis of the samples was carried out using a DTG-60H derivatograph (Shimadzu, Kioto, Japan).

The real density of the starting materials was determined using a Le Chatelier instrument. The bulk density was determined by filling a vessel with a capacity of 1000 cm^3. The average density was determined as the ratio of the sample mass to its volume. The materials’ sorption capacity was studied by keeping them in desiccators at different humidity levels and for different times. Their solubility determined the activity of the synthesized mineral additive in a 20% KOH solution. Determination of the amount of cohesive lime was determined following the Russian State Standard GOST 22688-2018 "Lime for building purposes". Test methods to determine the total content of active CaO + MgO in calcium lime using a titration method based on the neutralization reaction of hydrated lime HCl:

$$CaO + 2HCl + H_2O = CaCl_2 + 2H_2O$$

The investigation of finishing layers for strength in compression and bending was researched using a setup developed by the authors on specimens 10 × 10 × 10 mm and 10 × 10 × 50 mm in size, respectively (Figure 1).

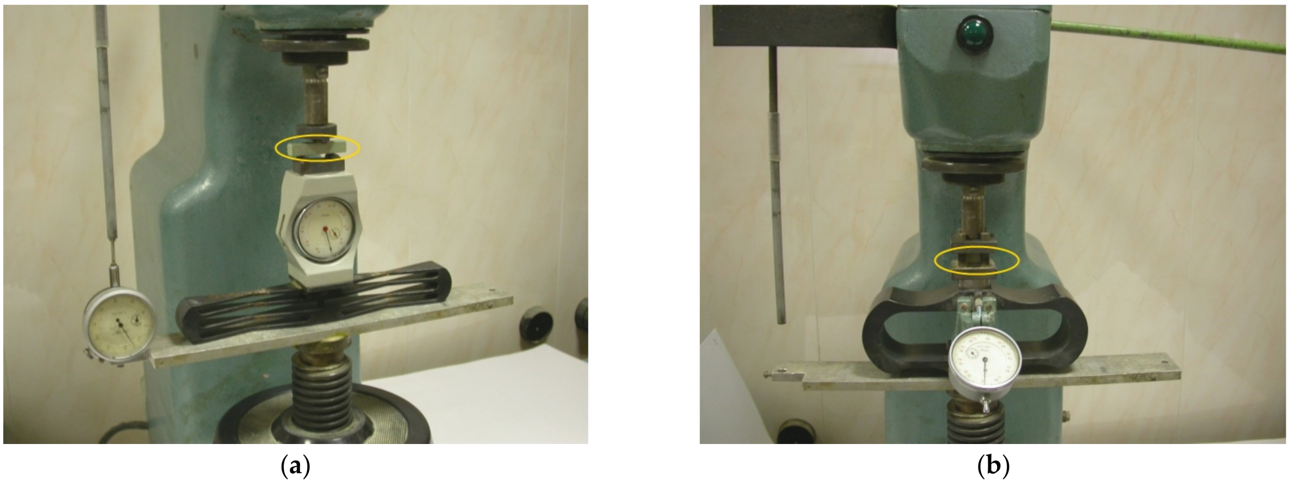
(a) (b)

Figure 1. Setup for determining the strength in bending (**a**) and compression (**b**).

The porosity was determined by the method of mercury porosimetry. Water absorption was determined according to the Russian standard GOST 5802-86 using 1 × 1 × 5 cm samples at the age of 28 days.

The water resistance was evaluated by the softening coefficient, which is equal to the ratio of the compressive strength of the material saturated with water to the compressive strength of the dry material:

$$K_s = \frac{R_s}{R_d}$$

The finishing mixes' water retention capacity was determined following the Russian State Standard GOST 5802-86.

3. Results and Discussion

3.1. Synthesis of Calcium Silicate Hydrates

In developing the technology for the production of the fillers, the following factors were considered: a density of the liquid glass, an amount of addition of the precipitant and the rate of its introduction, and a mode of drying the precipitate and the time of its storage. Table 3 shows that with an increase in the precipitate additive content during the filler synthesis, the lime compositions' compressive strengths with fillers increases.

It was found that the output of the filler synthesized from the water glass in the presence of $CaCl_2$ in the form of a 15% solution in an amount of 30 or 50% of the weight of liquid glass was 85%. This refers to the first set of specimens (liquid glass modulus 2.9). The output of the filler synthesized from the liquid glass in the presence of $CaCl_2$ in the form of 7.5% solution in the amount of 30 or 50% of the weight of liquid glass was 100%. After drying at a temperature of 105 °C, the filler's real density was 2200 kg/m^3, and the bulk density was 1935 kg/m^3.

Table 3. Dependence of the initial characteristics of the liquid glass on the properties of the modified composites.

Liquid Glass Silicate Modulus	Liquid Glass Density, kg/m^3	The Amount of the $CaCl_2$ Precipitation Additive Based on the Mass of Liquid Glass, %	Concentration of the Precipitating Additive Solution, %	Compressive Strength of the Lime Compositions in the Presence of CSH, MPa	CSH Output, %
2.9	1335	15	7.5	2.42 ± 0.127	54
			15	2.34 ± 0.124	55
		30	7.5	4.72 ± 0.256	100
			15	4.60 ± 0.245	85
		50	7.5	4.84 ± 0.272	100
			15	4.76 ± 0.268	85
		90	7.5	5.07 ± 0.298	90
			15	4.98 ± 0.296	67
1.53	1664	15	7.5	1.71 ± 0.106	38
			15	1.78 ± 0.107	36
		30	7.5	3.24 ± 0.208	55
			15	3.28 ± 0.208	53
		50	7.5	3.64 ± 0.234	95
			15	3.72 ± 0.237	88
		90	7.5	4.28 ± 0.264	85
			15	3.86 ± 0.243	70

It was revealed that the particle size distribution of the silicate-containing filler has a similar polyfractional nature; the size distribution of the filler particles is bimodal (Figure 2).

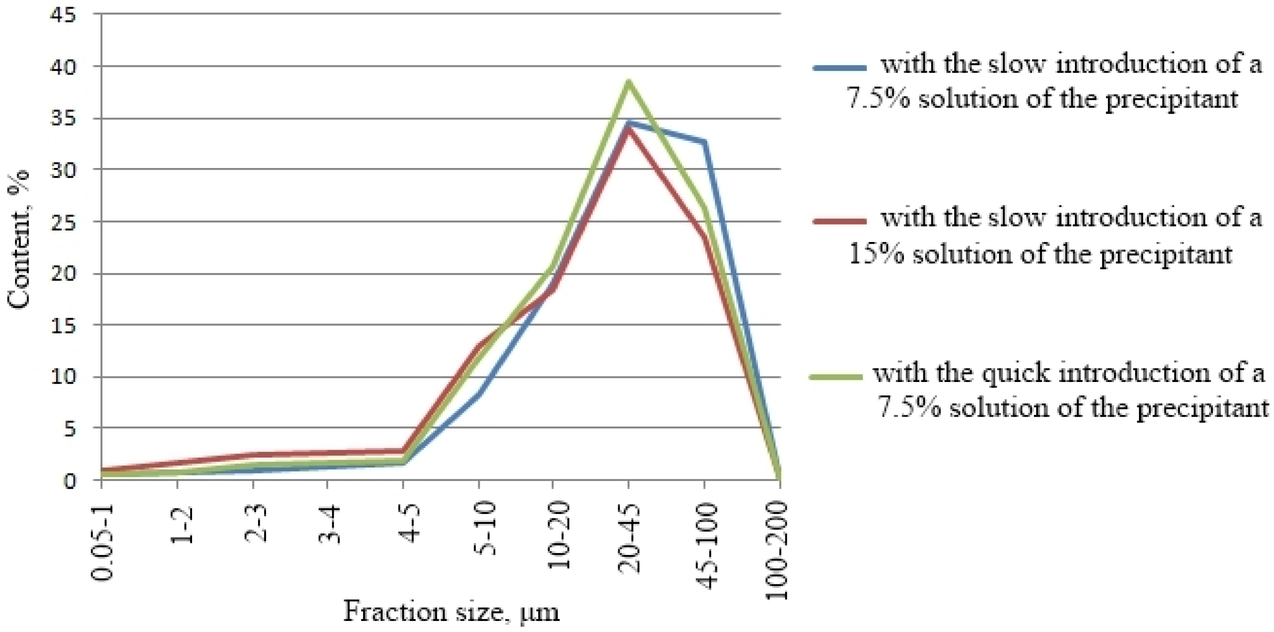

Figure 2. Granulometric composition of the fillers.

The slow introduction of the precipitant solution was carried out within 10 min, and the fast one was within 1 min. With the slow introduction of the $CaCl_2$ precipitating additive, a small number of large particles were formed in the sediment. The granulometric data indicate that particles with sizes of 20–45 μm prevail, the contents of which was in the range 34–39%. The arithmetic mean value of the filler's particle size synthesized with the slow introduction of the $CaCl_2$ precipitating additive was 29.35 μm.

The use of more dilute solutions (7.5%) led to a slowdown in precipitation and the appearance of larger crystals. The content of particles with a size of 45–100 µm was 32.62%, crystals with a particle size of 100–200 µm appeared, and their content was 0.04%.

With an increase in the sediment's maturation time, crystal growth was observed (Figure 3). The content of particles with a size of 45–100 µm increased to 33.21%. The content of particles with a size of 100–200 µm increased by 1.02%.

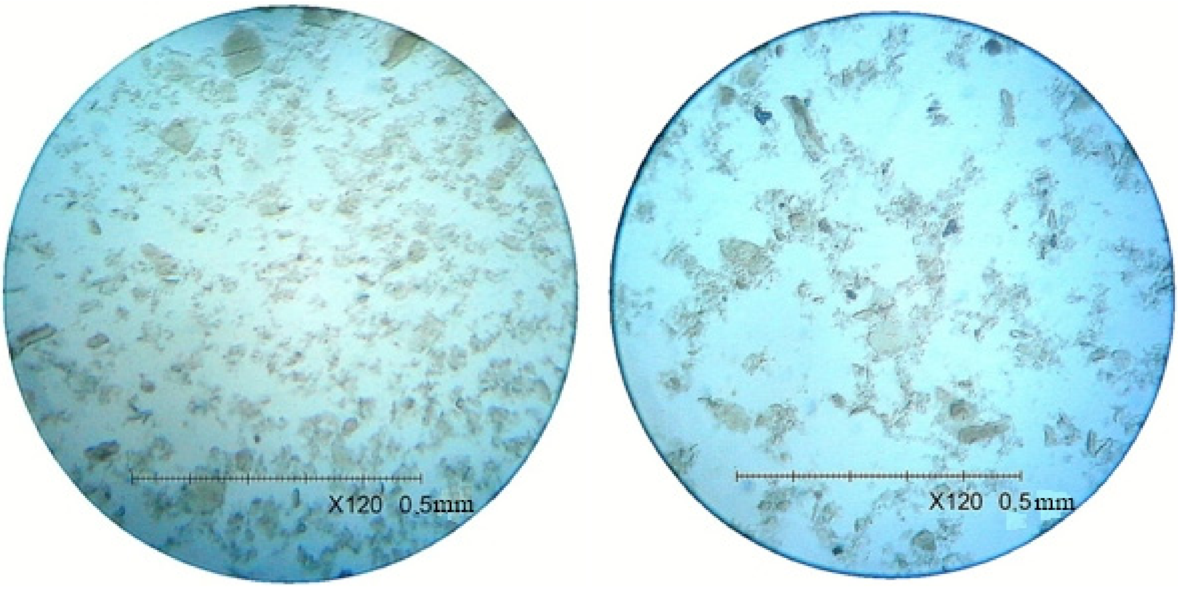

(**a**) (**b**)

Figure 3. Image of the crystals that matured for 2 (**a**) and 4 (**b**) days in the filtrate.

In studying the new growth's qualitative composition, it was found that the samples' degree of crystallization is low. The X-ray diffraction pattern (Figure 4) of the filler samples contains diffraction lines (Å) of the following compounds: calcium silicate hydrates of the tobermorite group (10.13059; 3.58269; 3.25556; 3.2579; 2.82015; 2.4662; 1.29764; 1.2618); solid solution CSH (B) in the form of slightly crystallized gel (4.76541; 3.03952; 2.82163) solid solution C–S–H (II): (2.22058; 1.87721; 1.41032); hydrohalites: (3.85831; 1.99449; 1.62748).

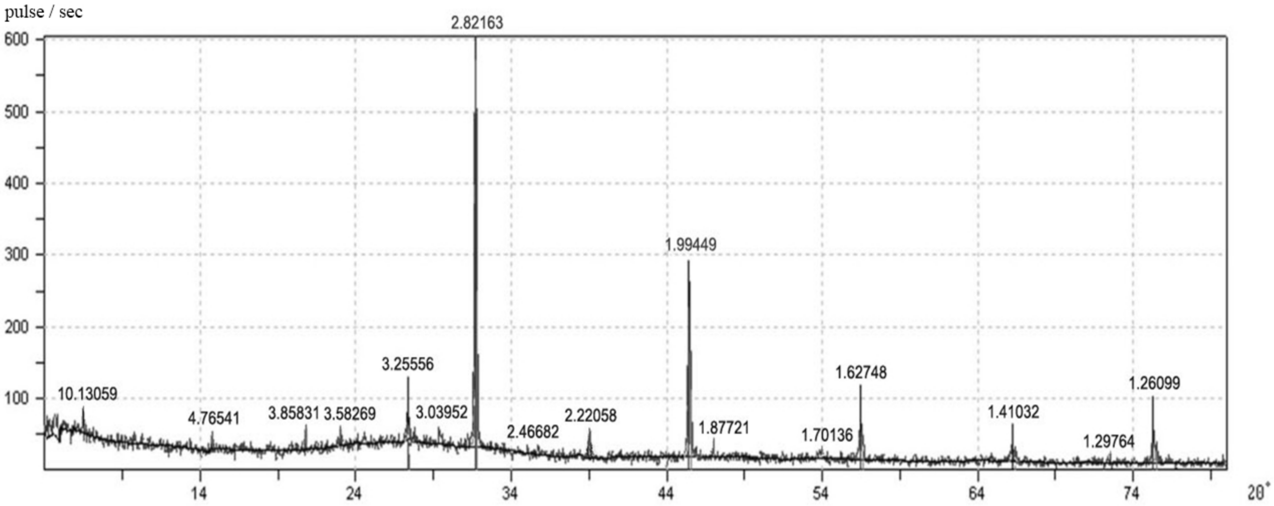

Figure 4. X-ray diffraction pattern of filler samples synthesized with the introduction of $CaCl_2$ additive in an amount of 50% of the mass of the water glass with a silicate modulus of 2.9.

The filler structure is represented by lamellar and acicular formations corresponding to calcium silicate hydrates (Figure 5).

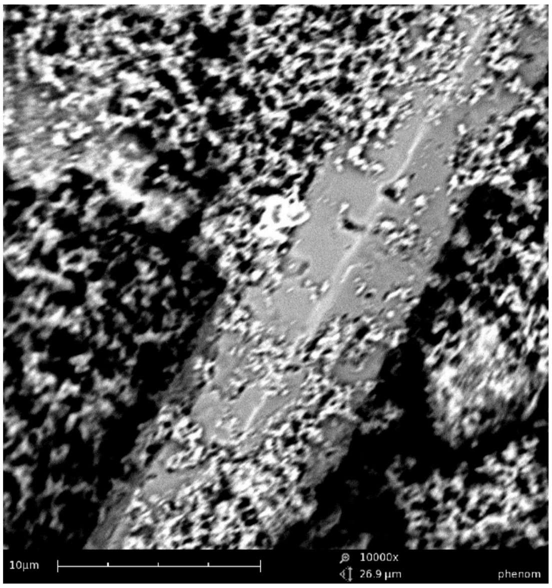

Figure 5. SEM image of the synthesized powder.

Analysis of the IR spectrum of the obtained filler's sample was performed for additional assessment. Figure 6 shows clearly distinguished absorption bands in the regions of 850–1100 cm^{-1}, 550–750 cm^{-1}, 400–550 cm^{-1}, confirming the presence of calcium silicate hydrates in the synthesized material.

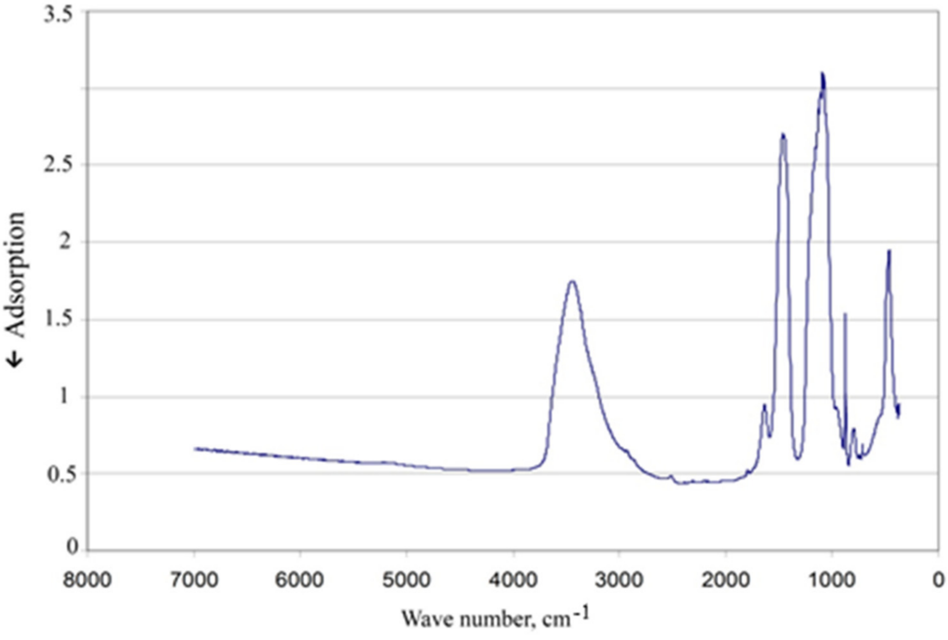

Figure 6. IR spectrum of the synthesized calcium silicate hydrates (CSH) filler sample.

The study of the hygroscopic properties of the fillers showed that they have a high sorption capacity. At a relative humidity of 72%, the sorption humidification after 10 days was 20%, and at a relative humidity of 100% it was 95%.

It was found that storage of the filler under conditions that exclude moisture access does not change its activity. After 20 days of storage under conditions excluding moisture access, the decrease in the activity of the filler was 5%, and after storage for 30–40 days it was 9–20%.

3.2. Development of the Modified Lime Compositions

The influence of the water–lime ratio (w/L), the content of modifying additives, the CSH filler, and the technology of its production on the properties of the finishing compositions was evaluated. It was revealed that the introduction of filler based on CSH into the lime composition changes the character of structure formation. A thermodynamic analysis of possible reactions was carried out during the interaction of the mix components (lime, filler based on calcium silicate hydrates, and mixing water) in accordance with the second law of thermodynamics (Table 4).

Table 4. Thermodynamic parameters of reactions in the interaction of the components of the mortar mix.

Chemical Formula	Heat of Formation ΔH^0_{298}, kJ/mol	Gibbs Energy ΔG^0_{298}, kJ/mol	Reactions
$Ca(OH)_2$	−63.3	−55.7	$CaO + H_2O = Ca(OH)_2$
$CaCO_3$	−114.7	−74.6	$Ca(OH)_2 + H_2O = CaCO_3 + H_2O$
$3CaO{\cdot}2SiO_2{\cdot}3H_2O$	−2757	−2439.4	$5CaO{\cdot}6SiO_2{\cdot}5H_2O + Ca(OH)_2 =$ $=3(3CaO{\cdot}2SiO_2{\cdot}3H_2O)$

The calculation results indicate the probability of all considered reactions proceeding in the forward direction (negative values of ΔH^0_{298}). The large numerical value ΔG^0_{298} found for the formation reaction makes it possible with sufficient probability to speak about the possibility of the reaction proceeding at standard temperature (25 °C) and at other temperatures.

In the study of solid-phase reactions occurring in the process of structure formation of lime compositions (Figure 7), it was revealed that in the samples of the lime composite with the synthesized filler there were diffraction lines (Å) of the following compounds: afwillites: 3.48012; 3.30452; 2.72286; 1.79241; 1.68957; 1.6027; portlandites: 2.62176; 1.48322; 1.44602; calcites: 2.28122; 1.9098; 2.49888; hillebrandites: 10.13052; 2.28122; 1.9242; 1.8730; okenites: 7.67421; 3.10452; 3.02709; tobermorites: 4.86172; 2.82723; 2.46761; calcium silicate hydroxides: 3.83385; 2.09187.

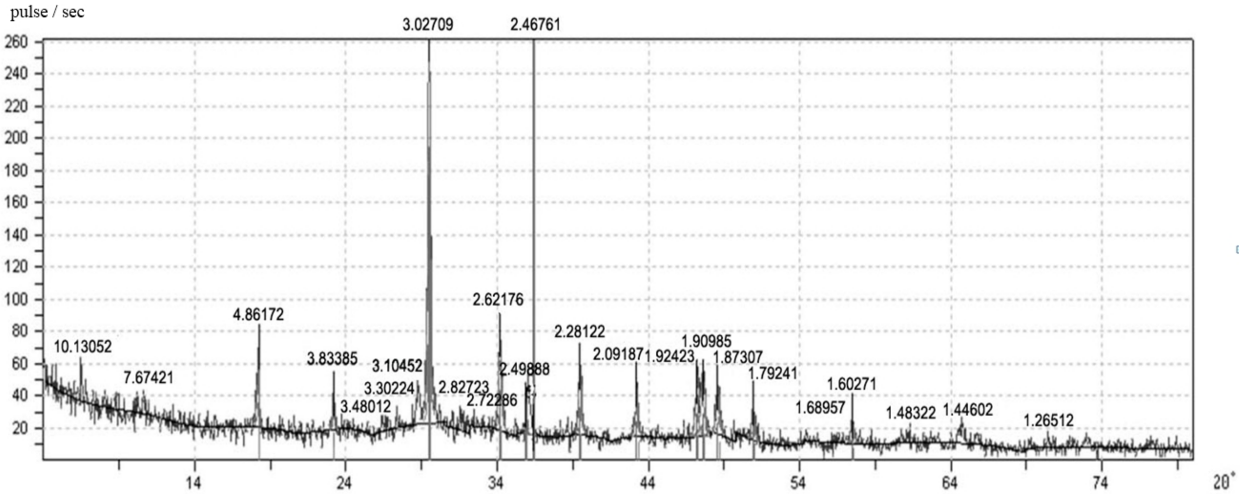

Figure 7. X-ray diffraction pattern of samples 03-A of a lime composite with a filler synthesized with the addition of $CaCl_2$ in an amount of 30% of the mass of the water glass with a silicate modulus of 2.9.

An increase in the number of peaks in the X-ray diffraction pattern of samples of a lime composite with filler based on CSH suggests that this filler was highly active and indicates a chemical interaction with lime. The studies carried out show that the CSH filler has a hydraulic activity of 178–289 mg/g depending on the synthesis mode. It was found that the amount of free lime in the control samples after 28 days of air-dry hardening was

60%, and in the samples with the CSH filler of the composition lime: CSH = 1:0.3, w/L = 0.9–27%, which indicates about the chemical interaction of calcium silicate hydrates with lime (Figure 8).

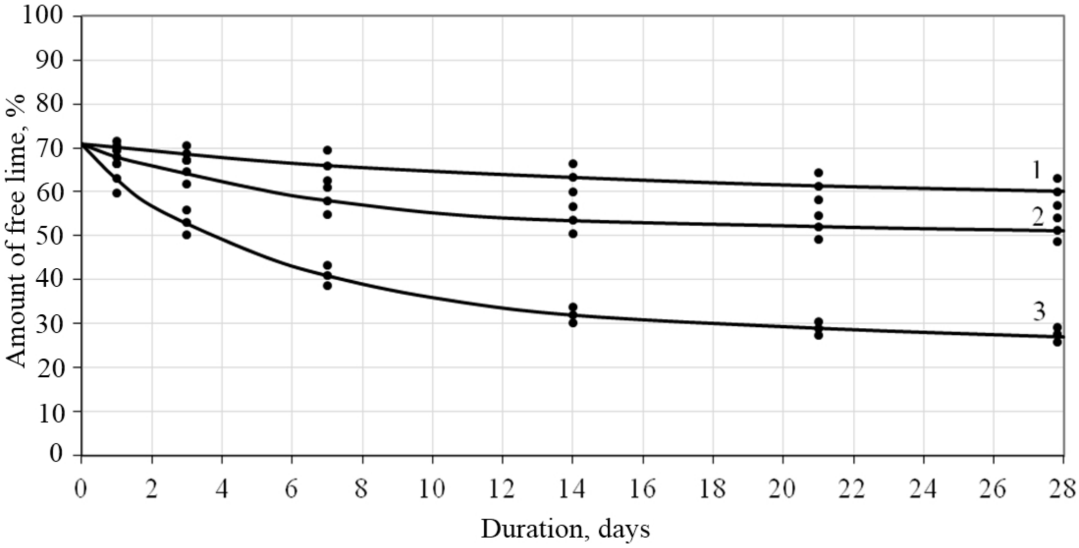

Figure 8. Decrease in the amount of free lime over time: 1—Ref-A; 2—03W-B; 3—03-B.

The data obtained were further confirmed during the differential thermal analysis (Figure 9).

It was found that in the samples of a lime composite with CSH filler, along with the decomposition of calcium oxide and calcium carbonate, dehydration of tobermorite (454.2 °C), afwilite (471.2 °C), hillebrandite (541.2 °C), okenite (645.7 °C) was observed, whose products are calcium silicates and modifications, wollastonite and crystobalite (Figure 9a). The total weight loss in the lime composite samples with the filler in the temperature range 400–700 °C was 26%, and in the control sample was only 5% (Figure 9b). A significant loss of water by weight in the samples of the lime composite with the filler suggests that a large number of highly basic calcium silicate hydrates were formed as a result of the chemical reaction of the filler and the lime.

The obtained XRD and DTA data indicate the formation of a stronger structure of the lime composite with CSH filler. Table 5 shows the compressive strength data of the lime composite depending on the filler content.

Table 5. Strength of the lime composite depending on the filler content.

Mix ID	Compressive Strength at 28 Days, MPa	Flexural Strength at 28 Days, MPa
Ref-A	1.62 ± 0.105	0.42 ± 0.027
Ref-B	1.56 ± 0.098	0.40 ± 0.023
005-A	3.96 ± 0.237	1.38 ± 0.086
005-B	3.24 ± 0.181	1.26 ± 0.068
015-A	4.56 ± 0.248	1.73 ± 0.109
015-B	3.82 ± 0.237	1.63 ± 0.089
03-A	4.56 ± 0.254	1.72 ± 0.110
03-B	3.62 ± 0.223	1.59 ± 0.085
03-D	3.55 ± 0.123	1.32 ± 0.110
05-B	4.31 ± 0.289	1.80 ± 0.112
05-C	3.82 ± 0.228	1.80 ± 0.110
05-D	3.33 ± 0.127	1.62 ± 0.112
03D-B	2.06 ± 0.123	0.72 ± 0.044
01-02D-B	3.46 ± 0.197	1.06 ± 0.068
02-01D-B	3.12 ± 0.179	0.96 ± 0.061

Table 5. *Cont.*

Mix ID	Compressive Strength at 28 Days, MPa	Flexural Strength at 28 Days, MPa
03W-A	2.06 ± 0.129	1.06 ± 0.068
03W-B	1.86 ± 0.121	0.96 ± 0.066
015W-A	1.93 ± 0.122	0.72 ± 0.044
015W-B	1.74 ± 0.104	0.71 ± 0.042
03SF-A	2.12 ± 0.135	1.34 ± 0.074
03SF-B	2.09 ± 0.123	1.18 ± 0.067
015SF-A	2.24 ± 0.118	1.14 ± 0.073
015SF-B	2.06 ± 0.112	1.05 ± 0.064

The highest values of strength indicators for modified compositions were ratios of lime:filler = 1:0.3 at w/L = 0.7 and lime:filler = 1:0.5 at w/L = 0.9.

An increase in the dispersion of the filler leads to an increase in its chemical activity and a regular increase in the values of the compressive strength (Table 6).

Table 6. Compressive strength of the lime composite depending on its specific surface area.

Specific surface area, cm^2/g	5896	7876	14,223
Compressive strength, MPa	3.64	4.56	6.28

Figure 9 shows the compressive strength values of lime paste during hardening. So, in 2 days, the compressive strength of lime paste with the CSH addition was 1.22 MPa, and for the reference composition was 0.36 MPa.

Based on the results shown in Figure 10, the models of the kinetics of hardening of the lime composites are proposed:

$$R = 0.86 \cdot t^{\frac{1}{2}} \tag{1}$$

$$R = 0.26 \cdot t^{\frac{1}{2}} \tag{2}$$

where R is a compressive strength of the lime composite; t is a hardening duration.

In order to regulate the rheological, technological, and functional properties of the finishing compositions, various superplasticizers were introduced into the mix formulation. The amount of the additive was 0.7–2% by weight of the binder. The use of superplasticizers S-3 or SP-3 gives the maximum plasticizing effect of the finishing lime composition. In this case, the water-reducing effect is 1.6 (Table 7). The introduction of the CSH filler to the lime increases the water-reducing effect to 1.8. The water-reducing effect is a reduction in water consumption while maintaining equal flowability.

Table 7. Values of the water-reducing effect depending on the composition of the mixes.

Superplasticizer	Additive Content, % by Weight of the Binder	Water-Reducing Effect	
		Ref-A	03-A
K	0.4	1.3	1.6
K	0.7	1.4	1.7
K	0.8	1.5	1.7
P-4	0.9	1.4	1.7
S-3	0.7	1.6	1.8
SP-3	0.7	1.6	1.8
F15G	0.4	-	-
1641F	0.2	-	-
F15G	2	1.5	1.7
1641F	1.5	1.5	1.8

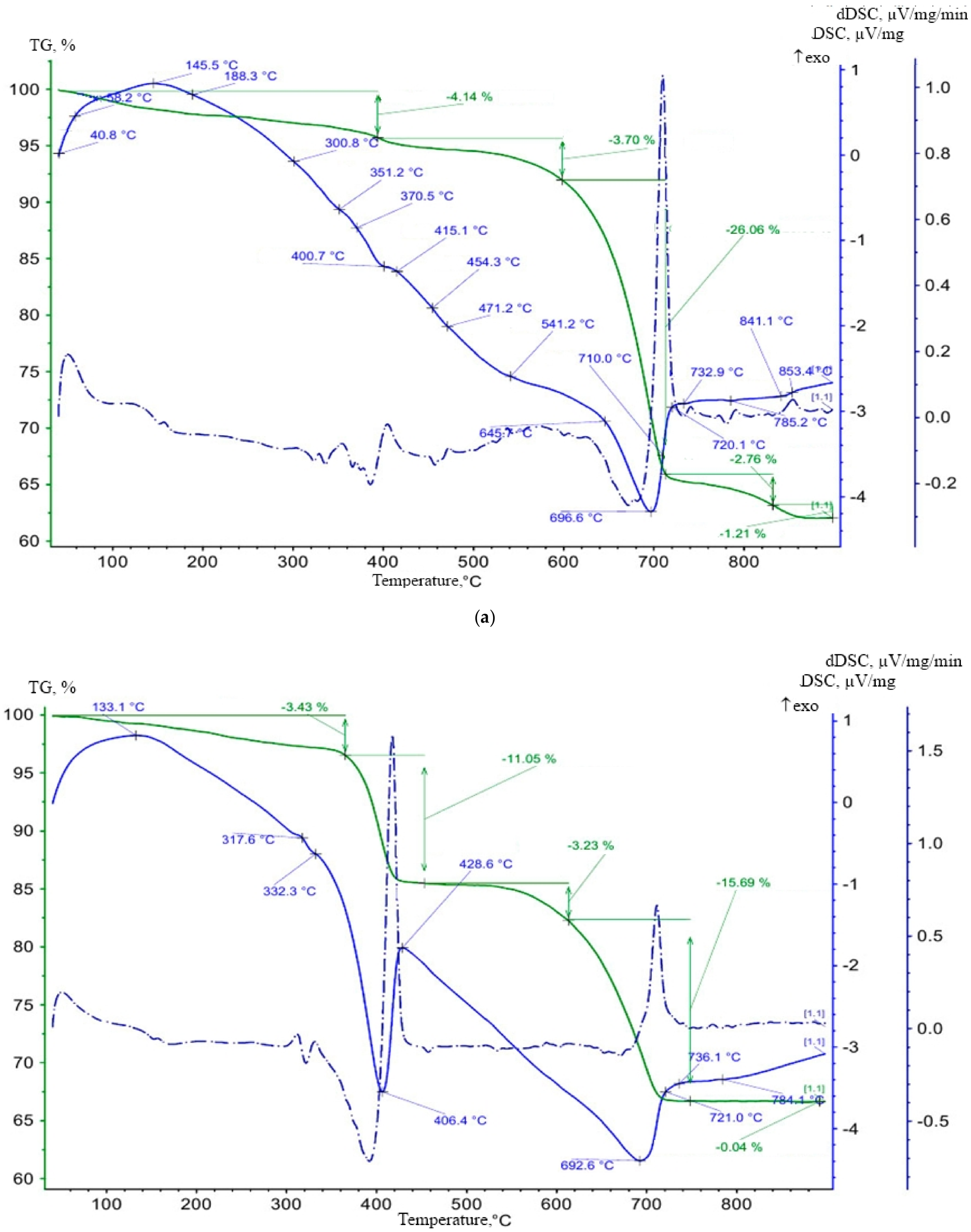

(**a**)

(**b**)

Figure 9. DTGA patterns of lime composites: (**a**) Ref-A; (**b**) 03-A.

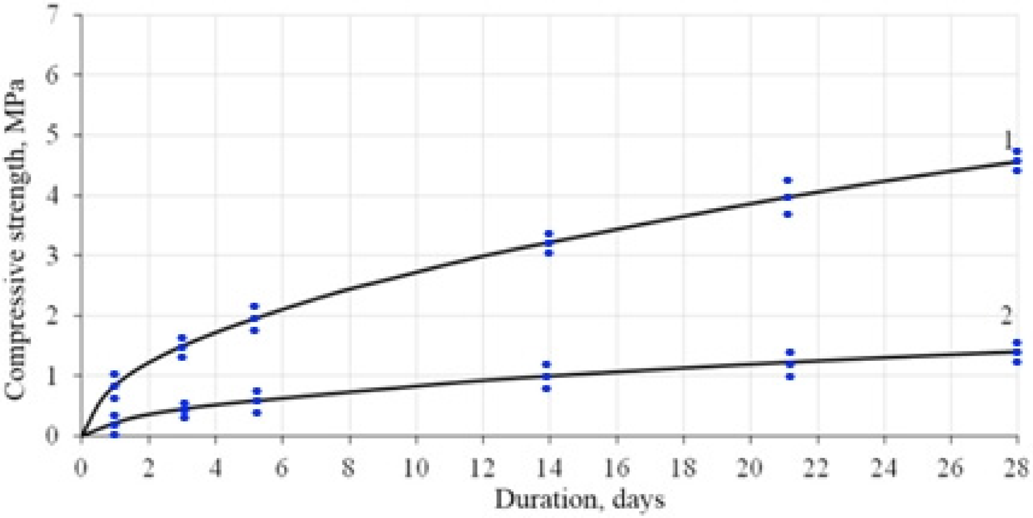

Figure 10. Kinetics of lime paste compressive strength gain: 1—03-A; 2—Ref-A.

The research results showed that the plasticizing effect, depending on the type of additive, persists for 1–2 h. The plasticizing effect was not observed at low dosages of the additives F15G (0.2–0.4%) and 1641F (0.2%). At the maximum dosage recommended by additive manufacturers, the water-reducing coefficient in CSH formulations was 1.7–1.8.

The filler's introduction into the lime composition increased the water retention capacity up to 96%. The superplasticizer's introduction into the lime composition with the CSH filler increased the water retention capacity to 99% (Table 8).

Table 8. Water retention capacity of the lime composites with the CSH filler.

Composition	Water Retention Capacity, %
lime:CSH = 1:0.3, w/L = 0.9	94%
lime:CSH = 1:0.5, w/L = 0.9	96%
lime:CSH = 1:0.3, w/L = 0.9, S-3	95%
lime:CSH = 1:0.3, w/L = 0.5, S-3	99%

When evaluating the structure, it was found that lime compositions form coatings characterized by high porosity and a significant volume of open pores (Table 9).

Table 9. Characterization of the lime paste porous structure.

Mix ID	Total Porosity, %	Open Porosity, %	Closed Porosity, %	Water Absorption by wt, %
Ref-1	60	50	10	44
03-B	56	43	13	38

The introduction of the CSH filler into the lime formulation leads to a decrease in porosity and an increase in the volume of closed pores; as a result of this, water absorption of the lime paste decreases.

Low values of open porosity and high values of strength of the developed composites made it possible to achieve high softening coefficients (Figure 11).

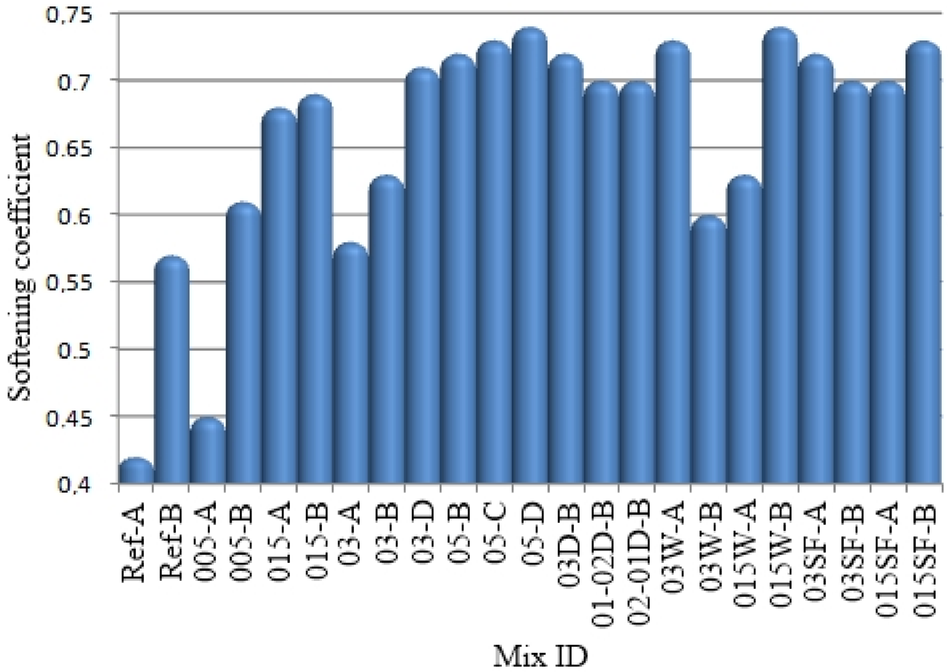

Figure 11. Softening coefficients of the developed composites.

4. Conclusions

For the first time, scientific data were obtained on the properties of the CSH filler and lime mixes with its use. Lime plaster composites with increased weather resistance have been developed, which is ensured by low values of open porosity and high values of strength. The resulting softening coefficient reaches 0.73, which is two times higher than the control unmodified composition. The following conclusions were drawn from the results of various tests:

(1). The regularities of the filler synthesis were established depending on a density, and silicate modulus of liquid glass, the amount of the precipitant additive, the rate of its introduction, and the drying mode. The rational content of the precipitating additive was found to be 30–50% of the mass of liquid glass in the form of a 7.5–15% solution. The rational density of liquid glass was determined, which is 1130–1663 kg/m^3, depending on a silicate modulus of liquid glass. The filler output was 85–100%, depending on the synthesis conditions.

(2). The phase composition of the filler, characterized by the presence of calcium silicate hydrates of the tobermorite group, a solid solution CSH (B) in the form of a weakly crystallized gel, a solid solution of C–S–H(II), hydrohalites, and calcites, was revealed. It was shown that the curves of the particle size distribution of the silicate-containing filler are of a polyfraction nature. The average particle diameter is 28–34 μm, depending on the filler synthesis mode. It was found that the filler based on calcium silicate hydrates has a high sorption capacity of 95% at 100% air humidity.

(3). The chemical interaction of the CSH filler with lime was established. It was shown that the filler based on calcium silicate hydrates has a hydraulic activity of 178–289 mg/g, depending on the synthesis mode. It was found that an amount of free lime in the lime composites was reduced by more than two times in the presence of CSH additive.

(4). It was revealed that lime compositions with CSH are characterized by a higher rate of strength development in comparison with the reference compositions. A mathematical model of the kinetics of hardening of a lime composite based on the binder filled with CSH was obtained. The regularities of the change in the strength of the lime composite depending on the fineness of the filler grinding, its content, and an amount of mixing water was established. It was revealed that the introduction of

CSH to the lime composition leads to a decrease in porosity and an increase in the volume of closed pores of the composite.

(5). The regularities of changes in the rheological and technological properties of lime finishing compositions were established depending on the conditions for the synthesis of the filler and its content, as well as the type of plasticizing additive. The introduction of the filler based on calcium hydrosilicates into lime promotes a 13–21% increase in the effect of plasticizing additives. The use of superplasticizers S-3 or SP-3 gives the maximum plasticizing effect of the finishing lime composition. In this case, the water-reducing effect is 1.8.

The prospects for further research should be considered in the direction of the possibility of obtaining organomineral, organic, and mineral additives for the modification of dry plaster mixes, expanding the range of local raw materials, and continuing research in the direction of studying the features of the structure formation processes of various finishing coatings.

Author Contributions: Conceptualization, V.L. and K.S.; methodology, R.F.; software, S.K.; validation, N.V., Y.V. and V.L.; formal analysis, K.S.; investigation, R.F.; resources, S.K.; data curation, N.V.; writing—original draft preparation, V.L., K.S., R.F., S.K., N.V. and Y.V.; writing—review and editing, V.L., K.S., R.F., S.K., N.V. and Y.V.; visualization, Y.V.; supervision, V.L.; project administration, K.S.; funding acquisition, R.F. All authors have read and agreed to the published version of the manuscript.

Funding: The research is partially funded by the Ministry of Science and Higher Education of the Russian Federation as part of World-class Research Center program: Advanced Digital Technologies (contract No. 075-15-2020-934 dated 17.11.2020).

Informed Consent Statement: Not applicable.

Data Availability Statement: The data presented in this study are available on request from the corresponding author.

Conflicts of Interest: The authors declare no conflict of interest.

References

1. Dylewski, R.; Adamczyk, J. The comparison of thermal insulation types of plaster with cement plaster. *J. Clean. Prod.* **2014**, *83*, 256–262. [CrossRef]
2. De Azevedo, A.R.G.; Alexandre, J.; Zanelato, E.B.; Marvila, M.T. Influence of incorporation of glass waste on the rheological properties of adhesive mortar. *Constr. Build. Mater.* **2017**, *148*, 359–368. [CrossRef]
3. Groot, C.; Van Hees, R.; Wijffels, T. Selection of plasters and renders for salt laden masonry substrates. *Constr. Build. Mater.* **2009**, *23*, 1743–1750. [CrossRef]
4. Murmu, M.; Singh, S.P. Strength characteristics of lime-activated slag cement. *Adv. Cem. Res.* **2015**, *27*, 268–277. [CrossRef]
5. Turanli, L.; Saritas, A. Strengthening the structural behavior of adobe walls through the use of plaster reinforcement mesh. *Constr. Build. Mater.* **2011**, *25*, 1747–1752. [CrossRef]
6. Yardim, Y.; Lalaj, O. Shear strengthening of unreinforced masonry wall with different fiber reinforced mortar jacketing. *Constr. Build. Mater.* **2016**, *102*, 149–154. [CrossRef]
7. Zimich, V. Magnesium Dry Mixes for Outer Wall Decoration. *Mater. Sci. Forum* **2016**, *870*, 3–7. [CrossRef]
8. Černý, R.; Kunca, A.; Tydlitát, V.; Drchalová, J.; Rovnaníková, P. Effect of pozzolanic admixtures on mechanical, thermal and hygric properties of lime plasters. *Constr. Build. Mater.* **2006**, *20*, 849–857. [CrossRef]
9. Fediuk, R.S. Mechanical Activation of Construction Binder Materials by Various Mills. In Proceedings of the IOP Conference Series: Materials Science and Engineering, Yurga, Russia, 26–28 November 2015; Volume 125, p. 012019.
10. Cultrone, G.; Sebastián, E.; Huertas, M.O. Durability of masonry systems: A laboratory study. *Constr. Build. Mater.* **2007**, *21*, 40–51. [CrossRef]
11. Lukuttsova, N.; Ustinov, A. Concrete modified by additive based on biosilicated nanotubes. *Int. J. Appl. Eng. Res.* **2015**, *10*, 40457.
12. D'Armada, P.; Hirst, E. Nano-Lime for Consolidation of Plaster and Stone. *J. Arch. Conserv.* **2012**, *18*, 63–80. [CrossRef]
13. Ibragimov, R.; Fediuk, R. Improving the early strength of concrete: Effect of mechanochemical activation of the cementitious suspension and using of various superplasticizers. *Constr. Build. Mater.* **2019**, *226*, 839–848. [CrossRef]
14. Pavlík, Z.; Fořt, J.; Pavlíková, M.; Pokorný, J.; Trník, A.; Černý, R. Modified lime-cement plasters with enhanced thermal and hygric storage capacity for moderation of interior climate. *Energy Build.* **2016**, *126*, 113–127. [CrossRef]

15. Salamanova, M.; Murtazaev, S.-A.; Alaskhanov, A.; Ismailova, Z.K. Development of Multicomponent Binders Using Fine Powders. In Proceedings of the International Symposium "Engineering and Earth Sciences: Applied and Fundamental Research" Dedicated to the 85th Anniversary of H.I. Ibragimov (ISEES 2019), Grozny, Russia, 10–13 June 2019; Atlantis Press: Amsterdam, The Netherlands, 2019.
16. Hauptmann, A.; Yalcin, U. Lime plaster, cement and the first puzzolanic reaction. *Paléorient* **2000**, *26*, 61–68. [CrossRef]
17. Loganina, V.I.; Simonov, E.E.; Jezierski, W.; Małaszkiewicz, D.; Loganina, L.V. Application of activated diatomite for dry lime mixes. *Constr. Build. Mater.* **2014**, *65*, 29–37. [CrossRef]
18. Fediuk, R.S.; Lesovik, V.S.; Liseitsev, Y.L.; Timokhin, R.A.; Bituyev, A.V.; Zaiakhanov, M.Y.; Mochalov, A.V. Composite binders for concretes with improved shock resistance. *Mag. Civ. Eng.* **2019**. [CrossRef]
19. Popov, O.; Moskalova, C. An analysis of the technological properties of facilitated plaster solutions made from dry building mixes. *Teh. Glas.* **2016**, *10*, 102–105.
20. Pahlavan, P.; Manzi, S.; Rodriguez-Estrada, M.T.; Bignozzi, M.C. Valorization of spent cooking oils in hydrophobic waste-based lime mortars for restorative rendering applications. *Constr. Build. Mater.* **2017**, *146*, 199–209. [CrossRef]
21. Hamard, E.; Morel, J.-C.; Salgado, F.; Marcom, A.; Meunier, N. A procedure to assess the suitability of plaster to protect vernacular earthen architecture. *J. Cult. Heritage* **2013**, *14*, 109–115. [CrossRef]
22. Asaad, M.A.; Ismail, M.; Khalid, N.H.A.; Huseien, G.F.; Raja, P.B. *Elaeis guineensis* leaves extracts as eco-friendly corrosion inhibitor for mild steel in hydrochloric acid. *J. Teknol.* **2018**, *80*. [CrossRef]
23. Zagorodnyuk, L.; Lesovik, V.; Sumskoy, D. Thermal insulation solutions of the reduced density. *Constr. Mater. Prod.* **2020**, 40–50. [CrossRef]
24. Vejmelková, E.; Keppert, M.; Rovnaníková, P.; Keršner, Z.; Cerny, R. Application of burnt clay shale as pozzolan addition to lime mortar. *Cem. Concr. Compos.* **2012**, *34*, 486–492. [CrossRef]
25. Tolstoy, A.D.; Lesovik, V.S.; Glagolev, E.S.; Krymova, A.I. Synergetics of Hardening Construction Systems. In *IOP Conference Series: Materials Science and Engineering*; IOP Publishing: Bristol, UK, 2018; Volume 327, p. 032056.
26. Walker, R.; Pavía, S. Physical properties and reactivity of pozzolans, and their influence on the properties of lime–pozzolan pastes. *Mater. Struct.* **2010**, *44*, 1139–1150. [CrossRef]
27. Zegardło, B.; Szeląg, M.; Ogrodnik, P. Ultra-high strength concrete made with recycled aggregate from sanitary ceramic wastes—The method of production and the interfacial transition zone. *Constr. Build. Mater.* **2016**, *122*, 736–742. [CrossRef]
28. Pogorelov, S.; Semenyak, G. Frost Resistance of the Steel Fiber Reinforced Concrete Containing Active Mineral Additives. *Procedia Eng.* **2016**, *150*, 1491–1495. [CrossRef]
29. Pu, X. Investigation on pozzolanic effect of mineral additives in cement and concrete by specific strength index. *Cem. Concr. Res.* **1999**, *29*, 951–955. [CrossRef]
30. Ezziane, K.; Kadri, E.H.; Hallal, A.; Duval, R. Effect of mineral additives on the setting of blended cement by the maturity method. *Mater. Struct.* **2009**, *43*, 393–401. [CrossRef]
31. Inozemtcev, A.; Korolev, E.; Qui, D.T. Study of mineral additives for cement materials for 3D-printing in construction. *IOP Conf. Ser. Mater. Sci. Eng.* **2018**, *365*, 032009. [CrossRef]